Communication

Molecular Dynamics Simulation of the HOONO Decomposition and the HO/NO Caged Radical Pair in Water

Hakan Gunaydin, and K. N. Houk

J. Am. Chem. Soc., **2008**, 130 (31), 10036-10037 • DOI: 10.1021/ja711365e • Publication Date (Web): 10 July 2008

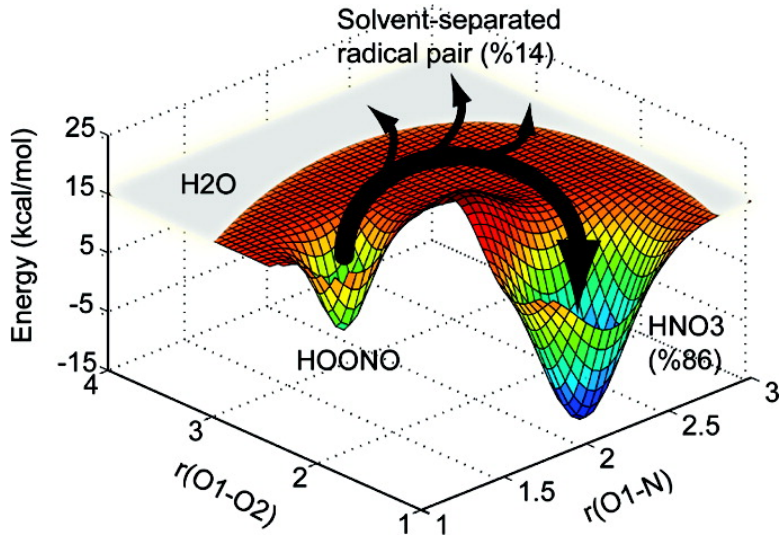

More About This Article

Additional resources and features associated with this article are available within the HTML version:

- Supporting Information
- Links to the 1 articles that cite this article, as of the time of this article download
- Access to high resolution figures
- Links to articles and content related to this article
- Copyright permission to reproduce figures and/or text from this article

View the Full Text HTML

Journal of the American Chemical Society is published by the American Chemical Society. 1155 Sixteenth Street N.W., Washington, DC 20036

J|A|C|S
COMMUNICATIONS

Published on Web 07/10/2008

Molecular Dynamics Simulation of the HOONO Decomposition and the $HO^{\bullet}/NO_2^{\bullet}$ Caged Radical Pair in Water

Hakan Gunaydin and K. N. Houk*

Department of Chemistry and Biochemistry, University of California, Los Angeles, California 90095

Received December 22, 2007; E-mail: houk@chem.ucla.edu

Nitric oxide is a small molecule with diverse roles in biology.[1] These include regulation of key physiological functions such as neurotransmission,[2] dilation of the blood vessels,[3] and the immune response.[4] Nitric oxide is also involved in the production of the strong oxidant, peroxynitrite ($ONOO^-$), in a diffusion-controlled reaction with superoxide in cells.[5]

Peroxynitrite, with a pK_a of 6.8,[6,7] is readily protonated to give peroxynitrous acid (HOONO) under physiological conditions. HOONO decays to nitrate with a half-life of ~1 s at room temperature.[7] The mechanism by which this transformation takes place has been the subject of an ongoing debate. In 1992, Koppenol et al. calculated the transition states (TS) and energetics ($\Delta G^{\ddagger}_{gas}$ = 17 kcal/mol) of the potential decomposition mechanisms using the semiempirical PM3 method.[8] These calculations supported a mechanism (Figure 1a) by which the nitric acid is generated from peroxynitrous acid via a loose three-membered cyclic TS. On the basis of the PM3 energetics, Koppenol et al. concluded that the decomposition of peroxynitrite occurs via this activated complex and that decomposition of HOONO via the homolysis of the peroxide bond (Figure 1b) does not compete.[8] In 2001, Goldstein et al. obtained a $\Delta G^{\ddagger}$ value of 16 kcal/mol for the decomposition of peroxynitrite.[9]

The decomposition of peroxynitrite generates a strong oxidant in solution with properties that are similar to those of the hydroxyl radical ($HO^{\bullet}$).[10] The three-membered loose TS, also called a high-energy intermediate, HOONO*, was speculated to account for the hydroxylation and nitration reactions, since the amount of the hydroxyl radical produced seemed to be insufficient to be accounted for by homolysis.

The decompositions of peroxynitrite and HOONO have been studied extensively. The kinetics of decay of peroxynitrite in the presence of CO_2 and methionine were reported to be second order.[6,11] This is evidence for the direct reaction of peroxynitrite with these substrates. On the other hand, oxidation rates of substrates such as dimethyl sulfoxide and deoxyribose by peroxynitrite are first order and only depend on the peroxynitrite concentration.[10] Although these first order rates were speculated to originate from the direct reaction of the substrates with the high energy intermediate, HOONO*,[8,10] the possibility of formation of a long-lived $HO^{\bullet}$ and NO_2 pair caged by the solvent water molecules ("caged radical pair") was also raised.[6]

The experiments of Merenyi et al. established that the HOONO decomposition occurred by formation of $HO^{\bullet}$ and NO_2.[12] Experiments showed that $HO^{\bullet}$ can be trapped during the decomposition of the HOONO by using high concentrations of $HO^{\bullet}$ scavengers such as deoxyribose and dimethyl sulfoxide; these give malondialdehyde and formaldehyde upon reaction with the $HO^{\bullet}$, respectively.[13] The yields of $HO^{\bullet}$ formed during the decomposition of HOONO range from 0−40%.[13,14] It is possible that the low yields of hydroxyl-derived products come from the reaction of HOONO

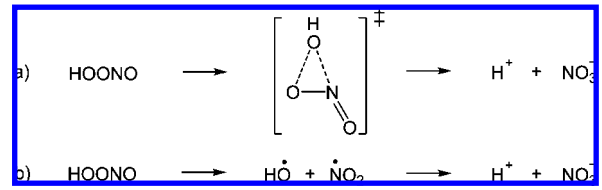

Figure 1. Decomposition of HOONO via HOONO* and homolysis.

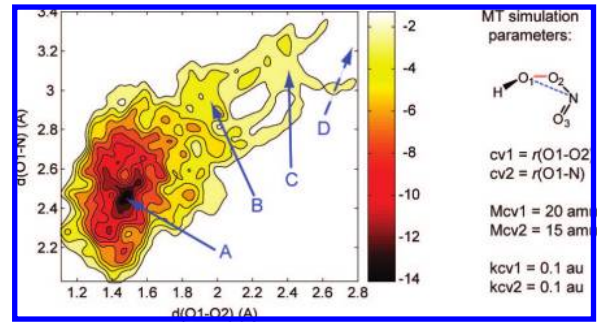

Figure 2. MT reconstructed free energy surface for the decomposition of HOONO (left) and MT simulation parameters (right).

with CO_2;[11,15,16] high yields might arise from the direct reaction of NO_2 with the $HO^{\bullet}$ scavenger.[13]

Homolysis activation free energies have been calculated for HOONO and its derivatives with various levels of theory in the gas phase. These calculations agree with the experimental activation free energy for the decomposition of HOONO.[15,17,18] In contrast to the initial PM3 energetics reported by Koppenol et al.,[8] the energy of the HOONO* was found to be significantly higher than $\Delta G^{\ddagger}$ required for homolysis of the peroxide bond of HOONO.[19] In the gas phase, formation of nitric acid from HOONO occurs via homolysis.[18] These gas phase calculations provide evidence against the formation of HOONO* and in favor of homolysis of the peroxide bond. However, the effect of water solvation could be profound, and the effect of a water cage on the lifetime of the $HO^{\bullet}/NO_2$ radical pair is not known.

We have applied the metadynamics (MT)[20] method to the determination of the lowest free energy reaction path for the decomposition of HOONO in water. MT simulations were run by using the CPMD Langrangian, and the electronic structure of the system was described with the UBLYP functional.[21] The MT parameters are given in Figure 2. The details of the calculations are given in the Supporting Information (SI). In this method, biasing potentials are introduced into the configurational space with collective variables to push the system out from the basin of attraction defining the solvated reactant, HOONO, into new basins of attractions (solvated intermediates or products).

The HOONO convex hull was filled by biasing potentials in about 6.5 ps. The MT simulation led to peroxide bond cleavage

10.1021/ja711365e CCC: $40.75

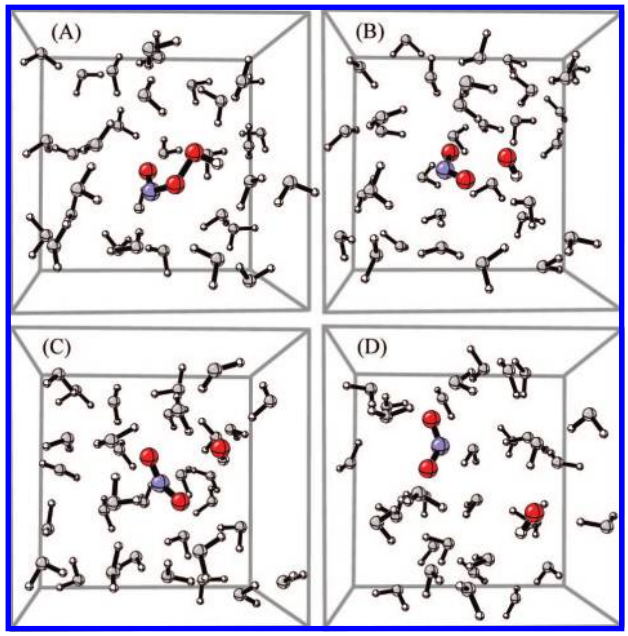

Figure 3. MT simulation determined snapshots for the homolysis of the HOONO in water: (A) HOONO, (B) TS, (C) caged radical pair, (D) solvent-separated radical pair.

with formation of $HO^{\bullet}$ plus NO_2, defined as $r(O1-O2) \geq 3.0$ Å. Two additional MT simulations began from the 5 ps MT simulation history. In these simulations, water molecules were randomly rotated with a maximum rotation amplitude of 15° and displaced with a maximum displacement amplitude of 0.2 Å in order to generate different starting configurations for trajectories. These two MT simulations also led to the formation of $HO^{\bullet}$ and NO_2 separated by water molecules. These simulations show that homolysis is the preferred minimum free energy pathway for the decomposition of HOONO in water. The free energy surface, reconstructed from the biasing potentials for the homolysis of the peroxynitrous acid around the HOONO convex hull, is shown in Figure 2. The full reconstructed FES is given in the SI. Figure 2 shows a local minimum in the region from $2.0 \leq r(O1-O2) \leq 2.8$Å. This region corresponds to a series of structures in which the $HO^{\bullet}$ and NO_2 are in close proximity. These two radical species are held together by the surrounding water molecules; this shallow local minimum arises because solvent reorganization is required for the separation of the hydroxyl radical and NO_2. According to the MT simulations, the homolysis activation free energy is 12.5 ± 0.6 kcal/mol. This value underestimates the experimental value of 16 kcal/mol. The discrepancy between the experimental value and MT computed value arises because the BLYP functional underestimates the endothermicity of the HOONO homolysis reaction by 3 kcal/mol (see SI for details) due to a variety of errors in this nonhybrid method. Additional errors could arise because of the choice of collective variables in the MT simulations. The results of the simulations can further be improved by using more accurate quantum mechanics, although the time for simulations is currently prohibitive.

Representative MT generated snapshots for HOONO in water (A), the TS that connects the HOONO to the caged radical pair (B), the regions that represent the caged radical pair (C), and the solvent-separated radical pair (D) are shown in Figure 3. The locations of these structures are marked in Figure 2. As seen in structure A, the minimum energy structure for HOONO in water is different from that found in the gas phase. While HOONO forms an intramolecular H-bond in the gas phase, it forms intermolecular H-bonds with the surrounding water molecules in water. The $O1-O2$ distances in structures represented by structures B and C are ca. 2.0 Å and between 2.0 and 2.8 Å, respectively.

No direct pathway from HOONO to nitrate was found. Instead, a caged radical pair is formed along the minimum free energy path. However, the dynamic fluctuations within the water cage connect the water-caged radical pair to the thermodynamic product, nitrate. CPMD simulations started from series of structures that correspond to the region C (Figure 2) showed that nitrate is formed from the water-caged radical pair 86% of the time and the water-caged radical pair gave solvent-separated radical pair 14% of the time. In these CPMD simulations, sampling of the geometries like those proposed for HOONO* was not observed and the caged radical pair collapsed to NHO_3 by radical pair coupling of the N−O bond.

Acknowledgment. We thank Prof. G. L. Squadrito for his valuable suggestions and the NIGMS-NIH Grant GM059446 for financial support of this research. This work was partially supported by the National Center for Supercomputing Applications under Grant CHE040013N and utilized the NCSA SGI Altrix supercomputer cluster.

Supporting Information Available: Details of the calculations and full FES for the HOONO decomposition. This material is available free of charge via the Internet at http://pubs.acs.org.

References

(1) Ignarro, L. J., *Nitric Oxide: Biology and Pathobiology*. Academic Press: San Diego, 2000.
(2) Bult, H.; Boeckxstaens, G. E.; Pelckmans, P. A.; Jordaens, F. H.; Van Maercke, Y. M.; Herman, A. G. *Nature* **1990**, *345*, 346–347.
(3) Pawloski, J. R.; Hess, D. T.; Stamler, J. S. *Nature* **2000**, *409*, 622–626.
(4) Bogdan, C. *Nat. Immunol.* **2001**, *2*, 907–916.
(5) Huie, R. E.; Padmaja, S. *Free Radical Res. Commun.* **1993**, *18*, 195–199. Nauser, T.; Koppenol, W. H. *J. Phys. Chem. A* **2002**, *106*, 4084–4086.
(6) Pryor, W. A.; Jin, X.; Squadrito, G. L. *Proc. Natl. Acad. Sci. U.S.A.* **1994**, *91*, 11173–11177. Pryor, W. A.; Squadrito, G. L. *Am. J. Physiol.* **1995**, *268*, L699–L722.
(7) Kissner, R.; Nauser, T.; Bugnon, P.; Lye, P. G.; Koppenol, W. H. *Chem. Res. Toxicol.* **1997**, *10*, 1285–1292.
(8) Koppenol, W. H.; Moreno, J. J.; Pryor, W. A.; Ischiropoulos, H.; Beckman, J. S. *Chem. Res. Toxicol.* **1992**, *5*, 834–842.
(9) Goldstein, S.; Czapski, G.; Lind, J.; Merenyi, G. *Chem. Res. Toxicol.* **2001**, *14*, 657–660.
(10) Beckman, J. S.; Beckman, T. W.; Chen, J.; Marshall, P. A.; Freeman, B. A. *Proc. Natl. Acad. Sci. U.S.A.* **1990**, *87*, 1620–1624.
(11) Lymar, S. V.; Hurst, J. K. *J. Am. Chem. Soc.* **1995**, *117*, 8867–8866.
(12) Merenyi, G.; Lind, J. *Chem. Res. Toxicol.* **1998**, *11*, 243–246. Merenyi, G.; Lind, J.; Goldstein, S.; Czapski, G. *Chem. Res. Toxicol.* **1998**, *11*, 712–713.
(13) Richeson, C. E.; Mulder, P.; Bowry, V. W.; Ingold, K. U. *J. Am. Chem. Soc.* **1998**, *120*, 7211–7219.
(14) Shi, X.; Lenhart, A.; Mao, Y. *Biochem. Biophys. Res. Commun.* **1994**, *203*, 1515–1521. Kissner, R.; Nauser, T.; Bugnow, P.; Lye, P. G.; Koppenol, W. H. *Chem. Res. Toxicol.* **1997**, *10*, 1285–1292. Pau, S.; Nguyen, S. Y.; Gladwell, T.; Rosen, G. M. *Biochim. Biophys. Acta* **1995**, *1244*, 62–68. van der Vliet, A.; O'Neill, C. A.; Halliwell, B.; Cross, C. E.; Kauer, H. *FEBS Lett.* **1994**, *339*, 89–92. Crow, J. P. C. S.; Chen, J.; Gunn, C.; Ischiropoulos, H.; Tsai, M.; Smith, C. D.; Radi, R.; Koppenol, W. H.; Beckman, J. S. *Free Radical Biol. Med.* **1994**, *16*, 331–338. Mahoney, L. R. *J. Am. Chem. Soc.* **1970**, *92*, 5262–5263. Yang, G.; Candy, T. E. G.; Baora, M.; Wilkin, H. E.; Jones, P.; Zazhat, N. B.; Saadalla-Nazhat, R. A.; Blake, D. R. *Free Radical Biol. Med.* **1992**, *12*, 327–330. Gerasimov, O. V.; Lymar, S. V. *Inorg. Chem.* **1998**, *38*, 4317–4321.
(15) Houk, K. N.; Condroski, K. R.; Pryor, W. A. *J. Am. Chem. Soc.* **1996**, *118*, 13002–13006.
(16) Merenyi, G.; Lind, J. *Chem. Res. Toxicol.* **1997**, *10*, 1216–1220.
(17) Olson, L. P.; Kuwata, K. T.; Bartberger, M. D.; Houk, K. N. *J. Am. Chem. Soc.* **2002**, *124*, 9469–9475. Olson, L. P.; Bartberger, M. D.; Houk, K. N. *J. Am. Chem. Soc.* **2003**, *125*, 3999–4006.
(18) Zhao, Y.; Houk, K. N.; Olson, L. P. *J. Phys. Chem. A* **2004**, *108*, 5864–5871.
(19) Sumathi, R.; Peyerimhoff, S. D. *J. Chem. Phys.* **1997**, *107*, 1872–1880. Bartberger, M. D.; Olson, L. P.; Houk, K. N. *Chem. Res. Toxicol.* **1998**, *11*, 710–711. Bach, R. D.; Dmitrenko, O.; Estevez, C. M. *J. Am. Chem. Soc.* **2003**, *125*, 16204–16205.
(20) Laio, A.; Parrinello, M. *Proc. Natl. Acad. Sci. U.S.A.* **2002**, *99*, 12562–12566.
(21) *CPMD;* Copyright IBM Corp 1990−2006*;* Copyright MPI für Festkörperforschung Stuttgart 1997−2001.

JA711365E